

Segmentation of Optic Cup and Disc for Diagnosis of Glaucoma on Retinal Fundus Images

Afolabi O. Joshua
Department of Electrical/Engineering
Science
University of Johannesburg,
Johannesburg, South Africa.
afolabij@uj.ac.za

Fulufhelo V. Nelwamondo
Modelling and Digital Science Unit,
Council for Scientific and Industrial
Research,
Pretoria, South Africa.
fnelwamondo@csir.co.za

Gugulethu Mabuza-Hocquet,
Modelling and Digital Science Unit,
Council for Scientific and Industrial
Research,
Pretoria, South Africa.
gmabuza@csir.co.za

Abstract— Glaucoma has been attributed to be the leading cause of blindness in the world second only to diabetic retinopathy. About 66.8 million people in the world have glaucoma and about 6.7 million are suffering from blindness as a result of glaucoma. A cause of glaucoma is the enlargement of the optic cup such that it occupies the optic disc area. Hence, the estimation of optic Cup to Disc ratio (CDR) is a valuable tool in diagnosing glaucoma. The CDR can be obtained by segmenting the optic cup and optic disc from the fundus image. In this work, an improved U-net Convolutional Neural Network (CNN) architecture was used to segment the optic disc and the optic cup from the fundus image. The dataset used was obtained from the DRISHTI-GS database and the RIM-ONE v.3. The proposed pipeline and architecture outperforms existing techniques on Optic Disc (OD) and Optic Cup (OC) segmentation on the Dice-score metric and prediction time.

Keywords—retinal fundus image, glaucoma, optic disc segmentation, cup to disc ratio, image segmentation.

I. INTRODUCTION

Glaucoma is a leading cause of blindness and often comes with no obvious symptoms. This has led to partial or complete loss of sight in its victims. Early detection is the only way to impede the effect of Glaucoma. Detection is usually carried out using the Cup-to-Disc-Ratio (CDR) measurement of the fundus. Though other field tests are also carried out to complement the CDR test. The segmentation of the optic cup and disc is usually carried out manually by trained professionals. The exercise is a tedious one influenced by emotional instability and fatigue [1]. The CDR for a non-glaucomatous fundus is expected to be less than 0.5 and greater than 0.5 for a glaucomatous fundus [2]. There have been several methods used to measure the CDR. The most common pipeline consist of (i) image pre-processing, (ii) Region of Interest (ROI) determination, (iii) optic-disc (OD) localization and finally optic-cup (OC) localization. This is the pipeline employed by [3-8] with little variations in the pipeline across the authors. The approach is computationally intensive when used on large batches of fundus since several iterations would be carried out on the fundus images. Furthermore, the accuracy of the pipeline depends greatly on the fundus image pixel intensity which varies across database or source of fundus image.

In this work, we present a model architecture that involves the use of CNN to segment the OD and OC. The dimensions of the segmented OC and OD can then be read off for the determination of absence or presence of glaucoma. The contributions of this research include a modified U-net architecture which has much less number of parameters than the known U-net, a segmentation pipeline that result to a high

dice score for OC and OD segmentation and a segmentation pipeline with a very low prediction time making the model suitable for batch prediction.

The rest of this paper is organized as follows: section II discusses the related work, section III discusses the proposed approach of the experiment, section IV presents the results of the experiment and the last section presents the conclusion.

II. RELATED WORK

Recent development in computer image recognition introduced the use of deep learning architectures and efficient algorithm for image segmentation. Convolutional Neural Network (CNN) [9] built on VGG-16 architecture [10] using transfer learning technique was proposed by Maninis [11] to segment OD and OC from fundus. The proposed method achieved a good dice score. OC segmentation is a more tedious task, this was done by Zilly *et al.* [7] using CNN with boosting, filtering of entropy [12], normalization of contrast and patches standardization. Zilly *et al.* also employed the use of AdaBoost algorithm [13] to train the filters. The proposed architecture was tested on the DRISHTI-GS database [14] and the RIM-ONE database [15] and a very high dice and Intersection-over-Union (IoU) score (both score metrics will be explained in section III) was achieved.

Built upon what was done in [7], Buhmann *et al.* [16] proposed a new technique which does not demand that the fundus image be cropped by the disc locations before it can segment OC location. Also, An entropy sampling technique to pick points with important information on the fundus image was proposed; a process that reduces computational complexity. A higher dice-score than [7] but a lower IoU score was achieved.

III. PROPOSED EXPERIMENTAL APPROACH

The approach proposed in this work is based on deep learning methods for segmenting the OC and the OD from the fundus image. This approach is proposed because of the proven excellent performance of CNN in image recognition task, its' simple framework, its' ability to generalize well with good accuracy and its' good performance on large batch-size predictions.

Fig.1 shows the OC and OD segmentation proposed pipeline. For the OC segmentation, the fundus images are cropped by the OD location (obtained from OD segmentation process). This is done so as to make the OC boundary more pronounced and detailed. The cropped images are scaled down using spline interpolation of the binomial order and resized to 128 x 128. The resizing is done to improve on the

training speed and also allow for more images per batch while training. Before feeding the images into the CNN, the contrast of the images is further improved by stretching out the most occurring intensity value in the images. This process improves the training process and allows model to learn better. The scikit-image histogram-equalization is used for this process. For the OD segmentation, the same process for the OC segmentation is followed except for the cropping process as indicated by the red jumper arrow. The proposed approach is further described by the following algorithm.

Step 1: RGB images cropping by the OD locations. This process is necessary for only OC segmentation and not OD segmentation

Step 2: Spline interpolation application to the RGB images using the binomial order and nearest mode of filling.

Step 3: Resizing the images to a 128X128 shape

Step 4: Applying histogram equalization to training images

Step 5: Images re-scaling. All values of images are set to be between 1 and 0. $x = x/255$

Step 6: Training the designed CNN model with the scaled images

The CNN architecture proposed is a modification and improvement on the U-Net [17] using Keras framework and tensor flow backend. U-Net has proven to perform well on OC and OD segmentation tasks having better results than sliding-window models. The CNN architecture proposed in this paper is shown in Fig.2. The proposed architecture has more convolutional layers but the same size of filters (i.e 3x3) in all layers except the output layer which has a filter size of 1x1. The proposed architecture has much less number of parameters than the earliest U-Net. Our experiment revealed that networks with large parameters over-fit quickly on the training data and therefore generalizes poorly for segmentation tasks. Batch-Normalization by Ioffe and Szeged [18] is used on each layer so as to bring the mean activation close to zero in all layers. Leaky version of the Rectified linear unit (ReLU) is used as the activation function ($f(x) = 0.018 * x$ for $x < 0$, $f(x) = x$ for $x \geq 0$) [19]. Leaky ReLU is used because it does not saturate and it makes the network to converge faster. The loss function used (1) has the same value as the dice-score.

$$C(X, Y) = -\log f(X, Y) \quad (1)$$

$$f(X, Y) = \frac{2 \sum_{i,j}^{h,w} x_{i,j} y_{i,j}}{\sum_{i,j}^{h,w} x_{i,j}^2 + \sum_{i,j}^{h,w} y_{i,j}^2} \quad (2)$$

where the probability that the pixels predicted is for the foreground is $X = (x_{i,j})$ and the given output is $Y = (y_{i,j})$, h, w are the height and width respectively.

$C(X, Y)$ has the same value as the conventional dice-score in (3). A similar metric to dice-score is the IoU score in (4). The IoU (4) is a metric used in segmentation task to quantify how much overlap exist between the target image and the predicted image. As shown in (4), it measures the pixels common to both the target image and predicted image and divides the common pixel by the individual pixels in the target and the predicted

image. Dice-score (3) is very similar to IoU only that it gives more incentive to every correct pixel in the predicted image by multiplying the pixels in both the target and predicted images by a factor of 2.

$$D(X, Y) = \frac{2|X \cap Y|}{|X| + |Y|} \quad (3)$$

$$I(X, Y) = \frac{|X \cap Y|}{|X \cup Y|} \quad (4)$$

The optimization of the model is done using the Stochastic Gradient Descent (SGD) with a momentum of 0.90 with nesterov for the OC segmentation and OD segmentation process. SGD is used because it gives a better result when compared to other optimizers



Fig.1 Proposed Pipeline for OC and OD segmentation

IV. EXPERIMENT RESULTS

The CNN is trained for 250 epochs for the OC and OD segmentation. The OC segmentation pipeline is trained and tested on the DRISHTI-GS and RIM-ONE v.3 database. Both database have 50 and 159 fundus images respectively. For training the CNN, 35 and 127 fundus images are used from

the DRISHTI-GS and RIM-ONE v.3 database respectively and the model is tested with 15 and 32 fundus images from the DRISHTI-GS and RIM-ONE v.3 database respectively. For OD segmentation only the RIM-ONE v.3 database is used.

The model is trained using Kaggle's 2 CPU cores, 14 GB RAM, 1 NVIDIA Tesla K80 GPU. A batch size of 8 and image size of 128 by 128 is used.

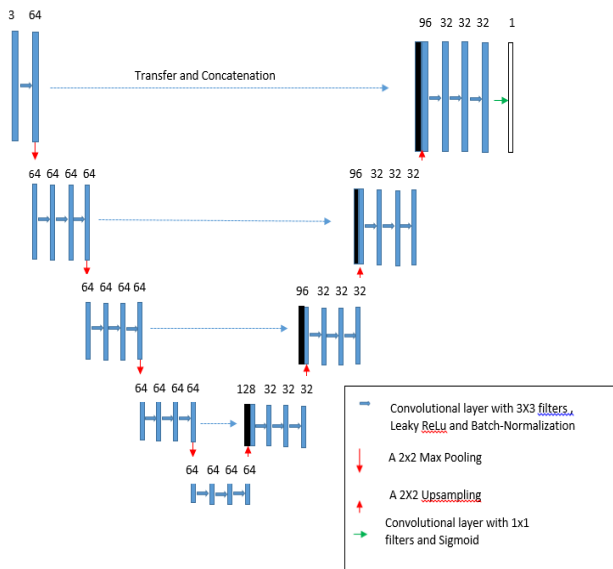


Fig.2 Proposed model architecture for OD and OC segmentation process

We compare our results with that of Artem [20], Zilly1 [16] and Zilly2 [7] and Maninis[11] using the dice-score in (3) and IoU score in (4) as our assessment. The results are presented in table I, II and III. Prediction time for our model is given by Kaggle's 2 CPU cores, 14 GB RAM, 1 NVIDIA Tesla K80 GPU. For Artem [20], it is given by Amazon Web services g2x2 large instance, 1 NVIDIA GRID GPU and a 2.66 GHZ quad-core CPU for Zilly [16].

TABLE I. OPTIC CUP (OC) SEGMENTATION RESULTS FROM DIFFERENT METHODS

	DRISHTI-GS			
	<i>IoU score</i>	<i>Dice Score</i>	<i>Prediction time(s)</i>	<i>Number of parameters</i>
Proposed Method	0.79	0.95	0.026	6.8×10^5
Artem	0.75	0.85	0.06	6.6×10^5
Zilly1	0.85	0.87	5.3	1890
Zilly2	0.86	0.83	-	-

TABLE II. OPTIC CUP (OC) SEGMENTATION RESULTS FROM DIFFERENT METHODS

	RIM-ONE v.3		
	<i>IoU score</i>	<i>Dice Score</i>	<i>Prediction time(s)</i>
Proposed Method	0.76	0.89	0.026
Artem	0.69	0.82	0.06
Zilly1	0.80	0.82	5.3

Fig. 3 and Fig. 4 show the predicted outputs of the proposed model and compares the best performance of the model with the worst performance of the model from the DRISHTI database for OC segmentation processes.

TABLE III. OPTIC DISC (OD) SEGMENTATION RESULTS FROM DIFFERENT METHODS

	RIM-ONE v.3			
	<i>IoU score</i>	<i>Dice Score</i>	<i>Prediction time(s)</i>	<i>Number of parameters</i>
Proposed Method	0.88	0.96	0.033	6.8×10^5
Artem	0.89	0.95	0.1	6.6×10^5
Zilly1	0.89	0.94	5.3	1890
Maninis[11]	0.89	0.96	0.13	1.85×10^7

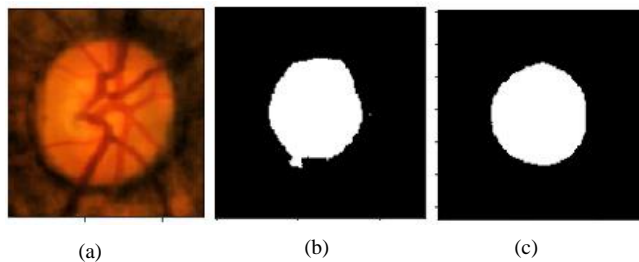


Fig. 3: Best OC segmentation. (a) Input image. (b) Predicted OC segmentation, (c) Correct OC segmentation.

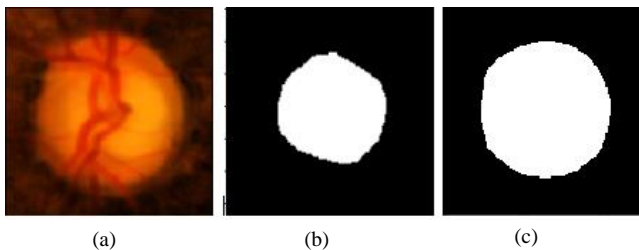


Fig.4: Worst OC segmentation (a) Input image. (b) Predicted OC segmentation, (c) Correct OC segmentation.

In Fig.3 (b), the predicted image has an IoU score of 0.87 and a dice score of 0.98.

The worst performance is shown in Fig. 4. The predicted image (Fig.4 (b)) has an IoU score of 0.66 and a dice score of 0.94.

Fig. 5 and Fig.6 show the predicted OC outputs from the RIM-ONE v.3 database for the best case and worst case respectively.

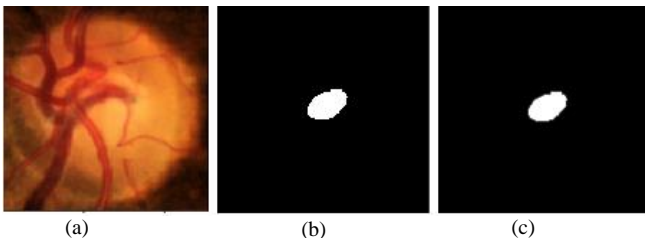


Fig.5: Best OC segmentation (a) Input image. (b) Predicted OC segmentation, (c) Correct OC segmentation.

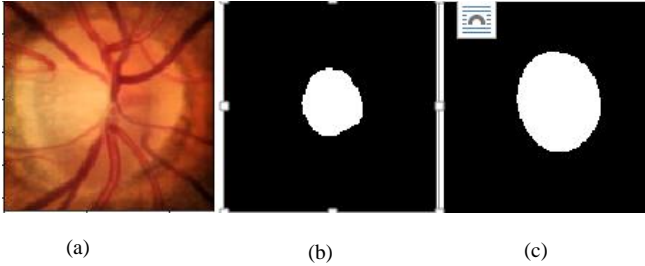


Fig.6: Worst OC segmentation (a) Input image. (b) Predicted OC segmentation, (c) Correct OC segmentation.

The best performance as shown in Fig.5 (b) has an IoU score of 0.99 and a dice score of 0.99 while the worst performance has shown in Fig. 6 (b) has an IoU score of 0.48 and a dice score of 0.67.

Fig. 7 and Fig.8 show the predicted OD output from the RIM-ONE v.3 database for the best case and worst case respectively.

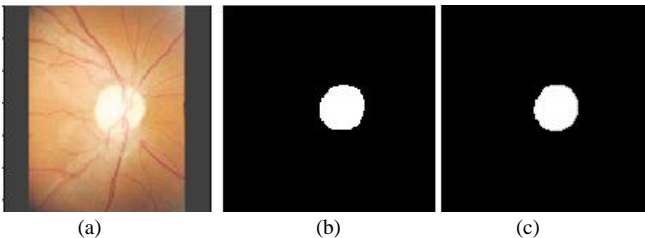


Fig.7: Best OD segmentation (a) Input image. (b) Predicted OD segmentation, (c) Correct OD segmentation.

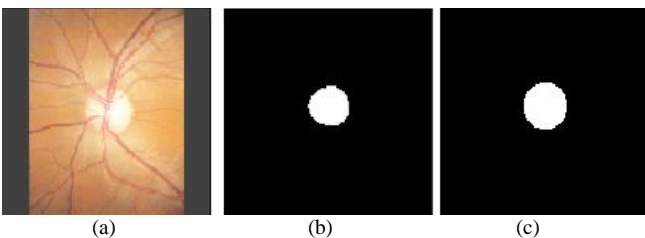


Fig.8: Worst OD segmentation (a) Input image. (b) Predicted OD segmentation, (c) Correct OD segmentation.

The best performance as shown in Fig.7 (b) has an IoU score of 0.95 and a dice score of 0.98 while the worst performance has shown in Fig. 8 (b) has an IoU score of 0.79 and a dice score of 0.90.

The results of our experimental work show that our model performed better than others in the dice-score and with very

little prediction time while having a comparative score in the IoU metric.

V. CONCLUSION

The proposed model pipeline achieved a very good performance for OC and OD segmentation as reflected by the IoU and dice scores. The proposed model can be used for batch predictions as well as online predictions. Hence, can be used on large number of fundus images and give results within short time. The OD segmentation was performed only on the RIM-ONEv3 database because the fundus images in the database have well defined OD boundary which is not so pronounced in fundus images from the DRISHTI database. However, fundus images from the RIM-ONEv3 database have difficult OC boundary lines thus causing OC segmentation process to have lower IoU and dice score when compared to scores from the DRISHTI database across all available models. The segmentation process for both OC and OD can be improved for a better IoU score.

REFERENCES

- [1] G. Lim *et al*, "Integrated optic disc and cup segmentation with deep learning," in Nov 2015, pp. 162-169. J. Clerk Maxwell, A Treatise on Electricity and Magnetism, 3rd ed., vol. 2. Oxford: Clarendon, 1892, pp.68-73.
- [2] S. K. S.Kavitha K.Duraiswamy, "Neuroretinal rim Quantification in Fundus Images to Detect Glaucoma," *International Journal of Computer Science and Network Security*, vol. 10, (6), pp. 134-140, 2010.
- [3]] A. Poshtyar, J. Shanbehzadeh and H. Ahmadi, "Automatic measurement of cup to disc ratio for diagnosis of glaucoma on retinal fundus images," in Dec 2013, Available: <https://ieeexplore.ieee.org/document/6746900>. DOI: 10.1109/BMEI.2013.6746900. R. Nicole, "Title of paper with only first word capitalized," J. Name Stand. Abbrev., in press.
- [4] H. Ahmad *et al*, "Detection of glaucoma using retinal fundus images," in Apr 2014, Available: <https://ieeexplore.ieee.org/document/6828388>. DOI: 10.1109/ICRETE.2014.6828388. M. Young, *The Technical Writer's Handbook*. Mill Valley, CA: University Science, 1989.
- [5] L. Shyam and G. S. Kumar, "Blood vessel segmentation in fundus images and detection of glaucoma," in Jul 2016, Available: <https://ieeexplore.ieee.org/document/7823982>. DOI: 10.1109/CSN.2016.7823982.
- [6] R. Panda *et al*, "Recurrent neural network based retinal nerve fiber layer defect detection in early glaucoma," in Apr 2017, Available: <https://ieeexplore.ieee.org/document/7950614>. DOI: 10.1109/ISBI.2017.7950614.
- [7] Zilly, Julian G.; Buhmann, Joachim M.; and Mahapatra, Dwarikanath. Boosting Convolutional Filters with Entropy Sampling for OpticCup and Disc Image Segmentation from Fundus Images. In: Chen X, Garvin MK, Liu JJ, Trusso E, Xu Y editors. Proceedings of the Ophthalmic Medical Image Analysis Second International Workshop, OMI 2015, Held in Conjunction with MICCAI 2015, Munich, Germany, October 9, 2015. 153-160. Available from <https://doi.org/10.17077/omia.1039>
- [8] Ji Sang Park, Hyeon Sung Cho and Jae Il Cho, "Automated extraction of optic disc regions from fundus images for preperimetric glaucoma diagnosis," in Oct 2017, Available: <https://ieeexplore.ieee.org/document/8204381>. DOI: 10.23919/ICCAS.2017.8204381.
- [9] E. Shelhamer, J. Long and T. Darrell, "Fully Convolutional Networks for Semantic Segmentation," *Tpami*, vol. 39, (4), pp. 640-651, 2017. Available: <https://ieeexplore.ieee.org/document/7478072>. DOI: 10.1109/TPAMI.2016.2572683.
- [10] K. Simonyan and A. Zisserman, "Very Deep Convolutional Networks for Large-Scale Image Recognition," 2014. Available: <http://arxiv.org/abs/1409.1556>

- [11] K. Maninis et al, "Deep Retinal Image Understanding," 2016. Available: <http://arxiv.org/abs/1609.01103>. DOI: 10.1007/978-3-319-46723-8_17.
- [12] R. C. Gonzalez, S. L. Eddins and R. E. Woods, Digital Image Processing using MATLAB. (2. ed., 7. repr. ed.) New Delhi [u.a.]: Tata McGraw Hill Education, 2012.
- [13] H. Doğan and O. Akay, "Using AdaBoost classifiers in a hierarchical framework for classifying surface images of marble slabs," Expert Systems with Applications, vol. 37, (12), pp. 8814-8821, 2010. Available: <https://www.sciencedirect.com/science/article/pii/S0957417410005233>. DOI: 10.1016/j.eswa.2010.06.019.
- [14] J. Sivaswamy et al, "Drishti-GS: Retinal image dataset for optic nerve head (ONH) segmentation," in Apr 2014, pp. 53-56.
- [15] F. Fumero et al, "RIM-ONE: An open retinal image database for optic nerve evaluation," in Jun 2011, pp. 1-6.
- [16] Zilly, Julian|Buhmann, Joachim M.|Mahapatra, Dwarikanath, "Glaucoma Detection Using Entropy Sampling And Ensemble Learning For Automatic Optic Cup And Disc Segmentation," Computerized Medical Imaging and Graphics, vol. 55, pp. 28-41, 2016. Available: <https://www.clinicalkey.es/playcontent/1-s2.0-S0895611116300775>. DOI: 10.1016/j.compmedimag.2016.07.012.
- [17] O. Ronneberger, P. Fischer and T. Brox, "U-Net: Convolutional Networks for Biomedical Image Segmentation," 2015. Available: <http://arxiv.org/abs/1505.04597>.
- [18] S. Ioffe and C. Szegedy, "Batch Normalization: Accelerating Deep Network Training by Reducing Internal Covariate Shift," 2015. Available: <https://arxiv.org/abs/1502.03167>.
- [19] A. Maas, Awni Y. Hannun and Andrew Y. Ng, "Rectifier nonlinearities improve neural network acoustic models," in Proceedings of the 30 Th International Conference on Machine Learning
- [20] A. Sevastopolsky, "Optic disc and cup segmentation methods for glaucoma detection with modification of U-Net convolutional neural network," Pattern Recognit. Image Anal, vol. 27, (3), pp. 618-624, 2017. Available: <https://search.proquest.com/docview/1938627054>. DOI: 10.1134/S1054661817030269.